Indian Journal of Science and Technology, Vol 10(11), DOI: 10.17485/ijst/2017/v11i10/110721, March 2017
ISSN (Print) : 0974-6846
ISSN (Online) : 0974-5645

Simulation and Analysis of Lead based Perovskite Solar Cell using SCAPS-1D

Usha Mandadapu[1], S. Victor Vedanayakam[1] and K. Thyagarajan[2]

[1]Department of Physics, Madanapalle Institute of Technology and Science, Madanapalle - 517325, Chittoor, Andhra Pradesh, India; ushakrishna7777@gmail.com, victorvedanayakams@mits.ac.in
[2]Department of Physics, JNTU College of Engineering Pulivendula - 516390, Andhra Pradesh, India; ktrjntu@gmail.com

Abstract

Objectives: Perovskite photovoltaic's are getting to be distinctly predominant option for the conventional solar cells achieving a maximum efficiency of 22.1%. This work is concerned about the design and analyses of lead-based perovskite solar cell model with the flexible architecture of lass/FTO/PCBM/$CH_3NH_3PbI_3$/PEDOT:PSS/Ag. **Method/Analysis**: The analysis of solar cell architecture is done using the Solar Cell Capacitance Simulator(SCAPS). It is a computer-based software tool and is well adapted for the analyses of homo and heterojunctions, multi- junctions and Schottky barrier photovoltaic devices. This software tool runs and simulates based on the Poisson's and continuity equation of electrons and holes. For this model, it is used to optimize the various parameters such as thickness, the defect density of absorber layer, doping concentrations(N_D and N_A) of Electron Transport Material (ETM) and Hole Transport Material (HTM). **Findings**: The thickness of $CH_3NH_3PbI_3$varied from 0.1µm to 0.6µm and the best results are observed at 0.3µm. The total defect density of the absorber varied from 10^{13} cm^{-3} to 10^{18} cm^{-3} and the minimum defect density of absorber layer is predicted as $10^{14}cm^{-3}$. The N_D or N_A of the HTM and ETM varied from 10^{14} to 10^{19} $cm^{-3}$and the PCE is maximum when N_D and N_A both kept at $10^{19}cm^{-3}$. By tuning the thickness of absorber layer and doping concentrations**,** the predicted results are as follows; maximum power conversion efficiency(PCE)31.77%, short circuit current density (J_{sc}) 25.60 mA/cm^2, open circuit voltage(V_{oc}) 1.52V, fill factor(FF) 81.58%. **Improvements:** With this proposed simulated model, the efficiency of the perovskite solar cell reaches to the 31%, which is an improvement of 4-5%, to the previous models, with the optimization of few material parameters. Hence this simulation work will provide the handy information in fabricating perovskite solar cells to reasonably choose material parameters and to achieve the high efficiency.

Keywords: Solar Cell, Perovskite, simulation, SCAPS, Efficiency

1. Introduction

$CH_3NH_3PbI_3$becomes a good light harvester due to its remarkable features such as ideal band gap, broad absorption spectrum, good cartrier transport mechanism, ease of fabrication on the flexible substrate and tunable band gap and long diffusion length[1–6]. Aforementioned features of lead halide perovskite material are encouraging to use in the fabrication of perovskite solar cell and becoming a good competitive material to the traditional silicon material[7–10]. At the beginning, the maximum PCE of these$CH_3NH_3PbI_3$ based perovskite solar cell is 3.8%[11]. In due course, by the novel methods of fabrication and the suitable selection of the architecture the PCE of perovskite solar cell has reached 22.1%[12]. Methylammonium lead halide perovskite materials are abundant on the earth and those are solution processable leading to the cost-effective fabrication technique. A Clear understanding of the underlying relation between the material features and the device architecture is needed to improve the performance of the device.

The architecture of the simulated model contains Poly(3,4-ethylene dioxythiophene):Poly(styrene sulfonate)(PEDOT:PSS),which is a common hole transport

*Author for correspondence

material in the perovskite-based solar cell. It is having a potential to use as an electrode on flexible substrates[13]. Some of the solvents like DMF, GBL, DMSO, which are being used in the preparation of perovskite solar cell, are modifying the properties of hole transport layer and it is essential to choose the suitable solvents which do not affect the conductivity of hole transport material, generally the conductivity of PEDOT:PSS changes from 10^{-3} S cm^{-1} to 10^{2} S cm^{-11} [14–15]. Appropriate doping of the PEDOT:PSS increases the number of holes and charge mobility.[6, 6]-Phenyl-C_{61}-butyric acidmethyl ester(PCBM) is widely used ETL in organic solar cells. PCBM material is P-type or N-type or intrinsic and in this architecture, PCBM is N-type having the majority number of electrons and medium holes[16].

From the literature, the related simulation work provided the basic knowledge to develop this model[17–21]. In this architecture, we studied and analyzed the effect of absorber layer properties(thickness, defect densities) and the influence of doping of HTM and ETM on the performance of the device.

2. Numerical Modelling and Device Simulation

A typical $CH_3NH_3PbI_3$ based solar cell structure consists of an absorber layer and at the top p-type(PEDOT: PSS) and n-type (PCBM) is arranged at the bottom side. The cell is illuminated schematically as shown in Figure 1.

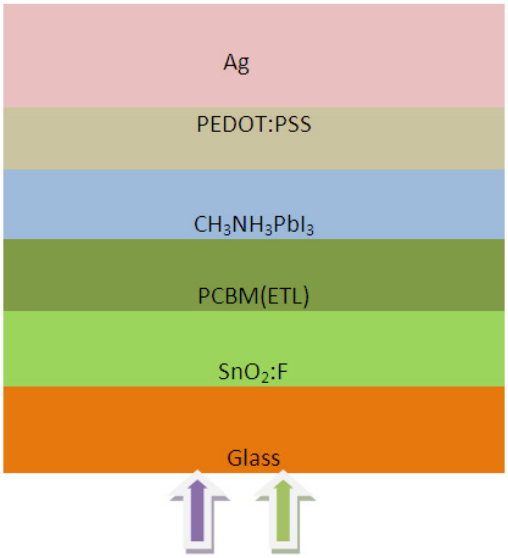

Figure 1. Schematic representation device architecture(Glass/FTO/PCBM/$CH_3NH_3PbI_3$/PEDOT:PSS/Ag).

SCAPS is a window application program, developed at the University of Gent with lab windows/CVI of the national instrument. The program organized in a number of panels in which the user can set the parameters or in which the results are calculated[22]. SCAPS analyses the physics of the model and it explains the recombination profiles, electric field distribution, carrier transport mechanism and individual current densities.

The continuity equations of electrons and holes are:

$$\frac{dj_n}{dx} = G - \mathbf{R} \quad (1)$$

$$\frac{dj_p}{dx} = G - R \quad (2)$$

where, j_n = Electron Current Density

j_p =Hole Current Density.

ϵ_r = Recombination Rate.

R = Generation Rate.

The Poisson equation is:

$$\frac{d\ \varnothing(x)}{dx} = \frac{e}{\epsilon\ \epsilon}(\rho(x) - n(x) + N_D - N_A + \rho_p\ \rho_n \quad (3)$$

$$g_D(E) = G_{Md}\exp[-(E - E_{pkd})\ /2\ _d \quad (3)$$

$$g_A(E) = G_{Ma}\exp[-(E - E_{Pka})^2 / 2\ _a^2$$

where, $\emptyset(x)$= Electrostatic potential

e = Electric Charge

ϵ_0 =Vacuum Permittivity

ϵ_r =Relative Permittivity

p and n are hole and electron concentration

N_D = Charged impurities of donor

N_A = Charged impurities of acceptor

ρ_p and ρ_n are holes and electron distribution

The Drift and Diffusion Equations are:

$$J_n = D_n \frac{dn}{dx} + \mu_n\, n \frac{d\emptyset}{dx}$$

$$J_p = D_p \frac{dn}{dx} + \mu_p\, p \frac{d\emptyset}{dx}$$

J_n =Electron current density

D_n = electron diffusion coefficient

μ_n =electron mobility

J_p = Hole current density

μ_p = Hole mobility

SCAPSsolves the Basic semiconductor equations in 1-Dimension under steady state condition. Figure 2

explains the simulation process using SCAPS.

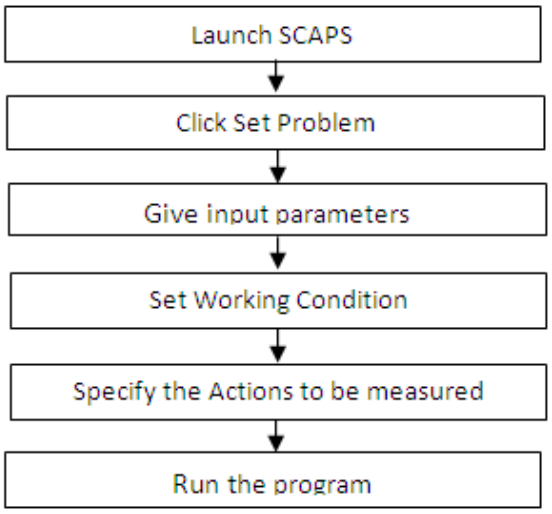

Figure 2. SCAPS working procedure.

Note that all simulation parameters for each layer in the architecture are carefully selected from those reported experimental data and other literature[23–27]. Table 1 summarizes all the primary parameters used in the simulation.

3.Output of Simulation studies

3.1 Influence of Absorber Layer Thickness on Solar Cell Characteristics

To absorb the maximum number of photons and to generate electron-hole pair, absorber layer should set for optimum thickness. The thickness of absorber layer has been varied from 0.1μm to 0.6μm. When the absorber layer thickness increases, the longer wavelength of illumination will produce a good amount of electron-hole pair generation. By reducing the absorber layer thickness, the depletion layer becomes very close to the back contact and more electrons will be captured by the back contact for recombination. By these fewer electrons will participate in the generation process, and finally, leads to the reduced fill factor and efficiency.

Figure 3 represents the variation of PV parameters with the thickness of absorber layer. The graph represents that the efficiency increases as we go from the thinner absorber to the thicker absorbers, due to the increased exciton generation. But there is a quick drop in the fill factor. The reason behind that is fill factor is strongly affected by the electric field and the electric field in the absorber decreases with increasing the forward bias. It will lead to reduced collection of carriers, which was assisted by the electric field. The higher fill factor needs quality absorber. By observing the Voc/thickness graph, we can say that there is a decrease in V_{oc} by increasing the thickness. Increased recombination in the thicker absorber layer leads to the reduced V_{oc}. From J_{sc}/thickness graph; short circuit current increases, by increasing the thickness. This is because the increase of spectral response at the longer wavelengths by increasing the thickness. When the thickness is varied from 0.1μm to 0.6μm, the efficiency increases upto 0.3μm, later it is decreased. Hence the optimized thickness of the absorber layer is 0.3μm. At this thickness the maximum power conversion efficiency is 31.07% and J_{sc}=25.59mA/cm^2, V_{oc}=1.51V, FF=80.04%.

Table 1. The parameters set for $CH_3NH_3PbI_3$ based solar cell at 300K and at A.M. 1.5G

Parameters	PEDOT:PSS	$CH_3NH_3PbI_3$	PCBM	SnO_2:F
Thickness(μm)	0.080	0.4	0.5	0.5
Band gap(eV)	2.2	1.55	2.100	3.5
Electron affinity(eV)	2.9	3.75	3.9	4.0
Dielectric permittivity(relative)	3.000	6.500	3.900	9.0
CB effective density of states(1/cm^3)	2.200E+15	2.200E+15	2.200E+19	2.200E+17
VB effective density of states(1/cm^3)	1.800E+18	2.200E+17	2.200E+19	2.200E+16
Electron thermal velocity(cm/S)	1.00E+7	1.00E+7	1.00E+7	1.00E+7
Hole thermal velocity(cm/S)	1.00E+7	1.00E+7	1.00E+7	1.00E+7
Electron mobility (cm^2/V.S.)	0.01	2.0	0.001	2.000E+1
Hole mobility (cm^2/V.S.)	0.0002	2.0	0.002	1.000E+1

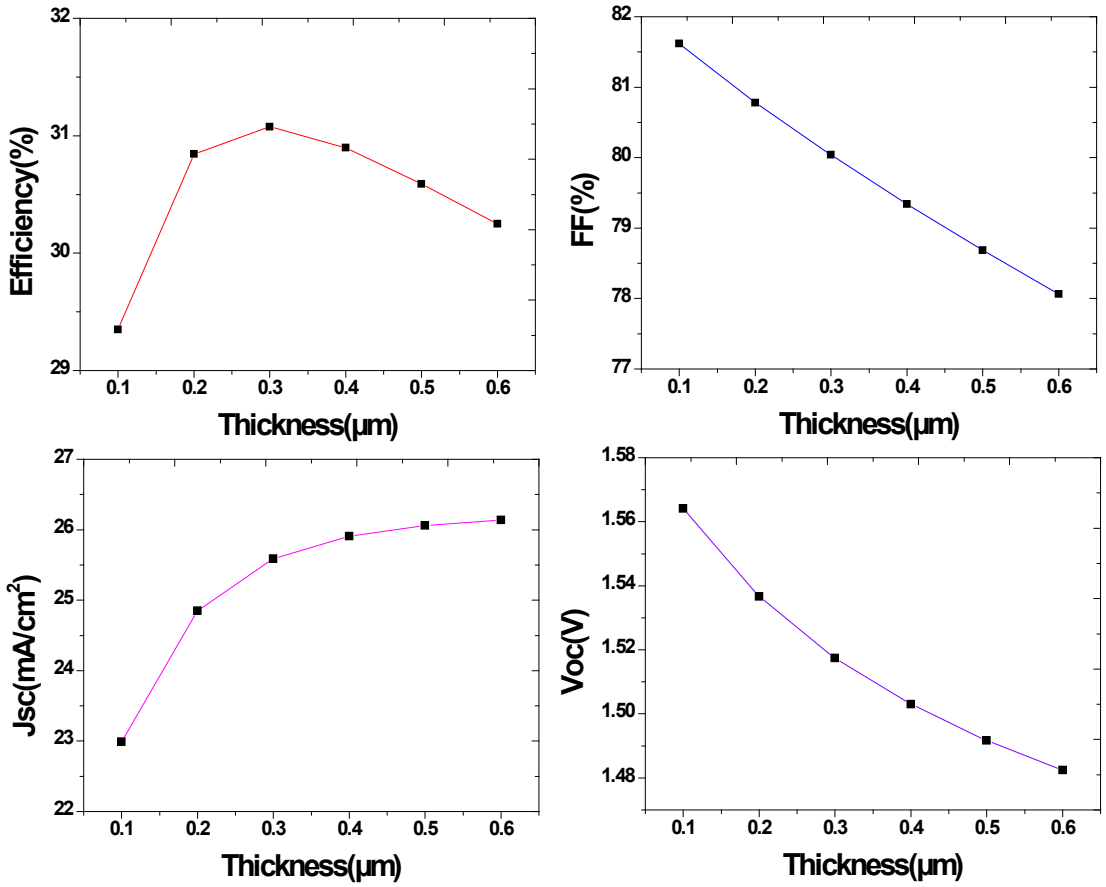

Figure 3. Variation of PV parameters by varying the thickness.

3.2 Effect of Defect Density (N_t)(cm^{-3}) of Absorber Layer on Photovoltaic(PV) Characteristics

Figure 4 represents the variation of PV parameters with the defect densities(cm^{-3}). Generation and recombination process occurs inside the absorber layer, so understanding the defect densities effect on the performance of the device is very important to reach maximum efficiency. Reduction in the quality of doping levels and the process of doping in the absorber layer is the main reason to form the defects and the device performance will be affected. The Gaussian distribution is a perfect method to understand the defect densities of absorber layer because a lot of defect energy levels are present in the perovskite layer[28] and the corresponding Gaussian distribution equations of acceptor and donor states are as follows:

$$-\frac{(E-E_{pkd})^2}{2\sigma_d{}^2}$$

$$-\frac{([E-E_{Pka})]^2}{2\sigma_a{}^2}$$

where, $g_{\downarrow}D\ (E) = G_{\downarrow}Md\ \exp[$

G_{Md} and G_{Ma} are effective defect densities

σ_d and σ_a are the standard energy deviations of the Gaussian and acceptor levels.

E_{PKD} and E_{Pka} are donor peak energy position measured positive from Ec and the acceptor peak energy position measured positive from Ev.

As can be clearly observed from the plots low-quality perovskite layer, with a huge number of defect densities and increased rate of recombination leads to the reduction in the diffusion length of charge carriers ultimately a life-

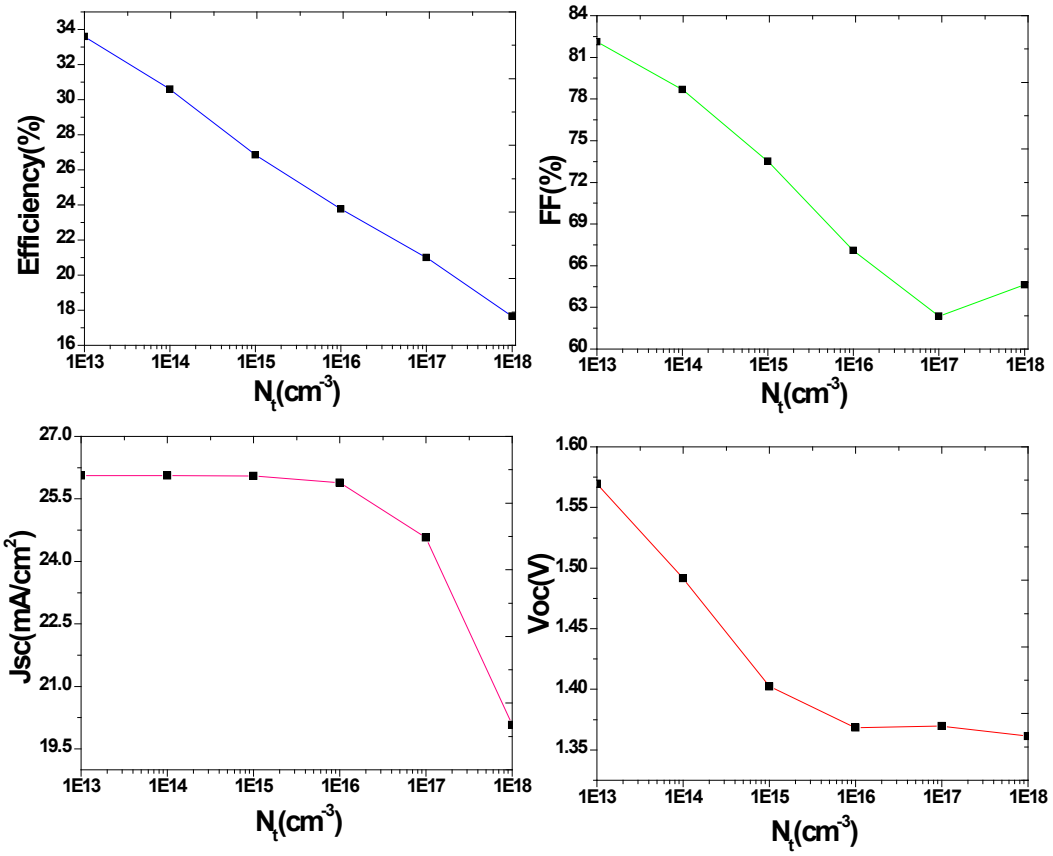

Figure 4. Variation of PV parameters by varying the defect density.

time of carriers will be decreased. Above all features has a significant influence on the performance of the device. We calculated the PV parameters by changing the defect densities from 10^{13} cm^{-3} to 10^{18} cm^{-3}. When the defect density is reached to 10^{18} cm^{-3}, the efficiency reaches to 17.66% but the less effect on V_{oc} i.e. 1.36V. In this model, the minimum number of defects in the absorber layer is predicted as 10^{14} cm^{-3}.

3.3 Influence of Doping of the ETM and HTM on the PV Parameters

Doping of a photoactive material in the solar cell architecture decides the electrical behavior of the layers which will affect the performance of the device. Proper doping of layers HTM and ETM enhances the interface electric field and improves the performance of the device. Doping of HTM and ETM can be done in two ways, one is doping with the minority carriers, which will largely reduce the fill factor, efficiency and the shape of J-V curve becomes S-shape. Another one is with the majority carriers, which leads to the improvement in fill factor and efficiency. With the moderate doping levels, an improved carrier transport and suitable energy position can be obtained. By the doping optimization and with the self-doping process deep defects can be avoided. To understand the doping effect of HTM and ETM on the device performance, the doping levels are varied from 10^{14} cm^{-3} to 10^{19} cm^{-3} and the graph. Figure 5 represents the changes in the PV parameters with the doping concentrations of HTM and ETM. Increased doping of layers HTM and ETM enhances the interface electric field between the HTM and ETM, this increased electric potential used to separate the excitons with less recombination rate and the performance of the device is increased. Alternatively, moderate doping is needed heavy doping leads to increased recombination and the perovskite semi-conductive nature changes to

metallic which obstructs the carrier transport mechanism[29]. Figure 5 represents the variation of PV parameters with the doping concentration(cm^{-3}) of HTM and ETM.

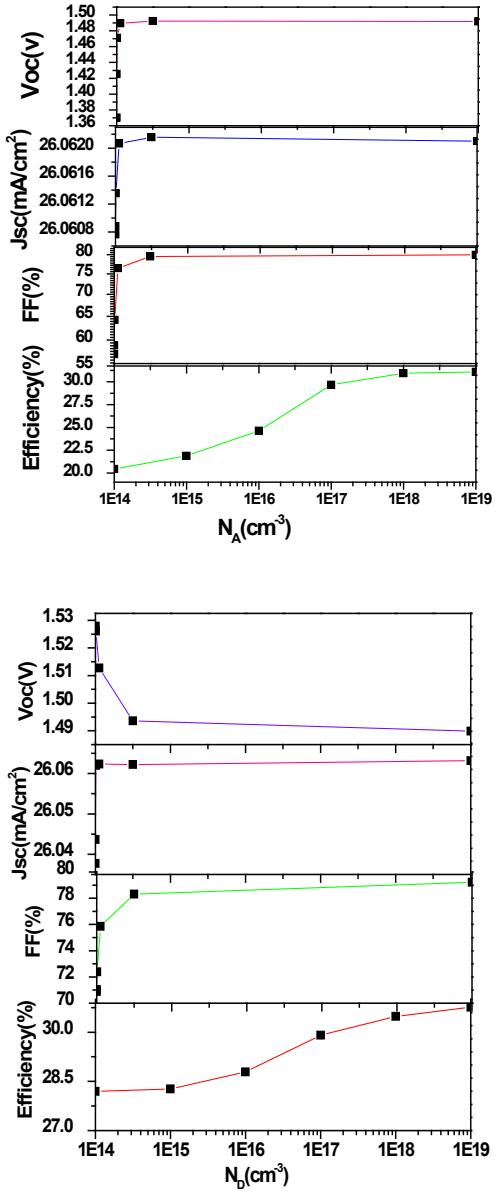

Figure 5. Variation of PV parameters by varying the doping density of ETM and HTM.

From the graph figure 5 donor concentration versus PV parameters, it was observed that Voc, FF, efficiency have been increasing, with an increase in donor density up to 10^{19} cm^{-3}. The reason behind that is by an increase of donor concentration the conductivity increases. Short circuit current density slowly decreases and it maintains a constant value. After the certain limit of donor concentration ($10^{15}cm^{-3}$), the PV parameters remains unchanged due to Moss-Burstein effect[30]. All the PV parameters are showing the best results when N_D and N_A both are keeping at 10^{19} cm^{-3}. At this doping concentration, the maximum power conversion efficiency is 31.77% and FF=81.58%, J_{sc}= 25.60mA/cm^2, V_{oc}=1.51V is obtained.

4. Current-Voltage Curve

Final J-V curve can be obtained by keeping all the optimized parameters in the designed model. The final model contains thickness of absorber layer as 0.3µm and the defect density is 10^{14} cm^{-3} and the doping levels of HTM and ETM are set as 10^{19} cm^{-3}. Figure 6 represents the final characteristic J-V curve of the simulated model with the all former optimized parameters.

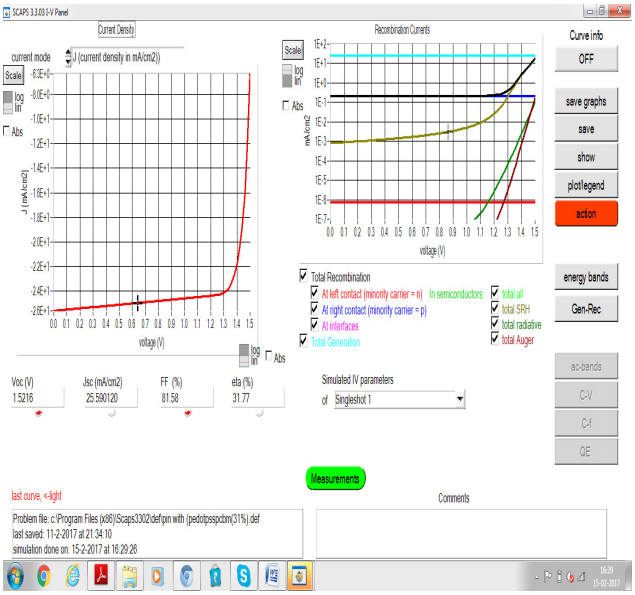

Figure 6. Simulated J-V curve.

5. Conclusion

The perovskite solar cell having the architecture Glass/FTO/PCBM/$CH_3NH_3PbI_3$/PEDOT:PSS/Ag is designed and analyzed using Solar cell capacitance simulator. Absorber layer thickness and defect density influence on the performance of the solar cell are investigated and the doping concentration of HTM and ETM effect on the PV, characteristics are observed. Moderate thickness and the absorber with the low defect are showing the better performance. The doping concentration of HTM, ETM are

showing the significant improvement on the PV parameters. After optimizing all the parameters and selecting the thickness of the absorber as 0.3 μm and the defect density as 10^{14} cm^{-3}, the doping concentrations of ETM and HTM are 10^{19} cm^{-3}. We got the power conversion efficiency is 31.77% and a good J_{sc} value (25.60mA/cm^2) is attained and the corresponding FF, V_{oc} is 81.58%, 1.52V.

6. Acknowledgements

The authors thank to Marc Burgelman and his team at the University of Gent for the access of SCAPS.

7. References

1. Dong Q, Fang Y, Shao Y, Mulligan P, Qiu J, Cao L, Huang J. Electron-hole diffusion lengths 175 mm in solution-grown CH3NH3 PbI3 single crystals. Science. 2015; 347(6225):968–70. Crossref
2. Chen Y, Peng J, Diqing S, Chen X, Liang Z. Efficient and balanced charge transport revealed in planar perovskite solar cells. ACS Applied Materials and Interfaces. 2015; 7(8):4471–5. Crossref
3. Hsiao YC, Wu T, Li M, Liu Q, Qin W, Hu B. Fundamental physics behind high-efficiency organo-metalhalide perovskite solar cells. Journal of Material Chemistry A. 2015; 3(30):15372–85. Crossref
4. Luo S, Daoud WA. Recent progress in organic-inorganic halide perovskite solar cells: Mechanisms and material design. Journal of Material Chemistry A. 2015; 3(17):8992–9010. Crossref
5. Mola GT. Enhanced photon harvesting in OPV using optical reflective surface. Applied Physics. A, Materials Science and Processing. 2015; 118(2):425–29. Crossref
6. Tessema G. Charge transport across bulk-heterojunction organic thin film. Applied Physics. A, Materials Science and Processing. 2012; 106(1):53–7. Crossref
7. Kazim S, Nazeeruddin MK, Grätzel M, Ahmad S. Perovskite as light harvester: A game changer in photovoltaic's. Angewandte Chemie International Edition. 2014 Mar 10; 53(11):2812–24. Crossref
8. Wayesh Q, Yesmin AJ, Gloria MD, Tashfiq M, Hossain MI, Islam SN. Optical analysis in CH3NH3PbI3 and CH3NH3PbI2Cl based thin-film perovskite solar cell. American Journal of Energy Research. 2015; 3(2):19–24.
9. Won LS, Kim S, Bae S, Cho K, Chung T, Mundt LE, Lee S, Park S, Park H, Martin CS, Stefan WG, Yohan K, Jun Y, Kang Y, Lee HS, Kim D. UV degradation and recovery of perovskite solar cells. Scientific Reports. 2016; 6(38150):1–10.
10. Yin WJ, Shi TT, Yan YT. Unusual defect physics in CH3NH3PBI3 perovskite solar cell absorber. Applied Physics Letters A. 2014 Feb; 104(6):063903-1–4. Crossref
11. Kojima A, Kenjiro T, Shirai Y, Miyasaka T. Organometal halide perovskites as visible-light sensitizers for photovoltaic cells. Journal of American Chemical Society. 2009; 131(17):6050–51. Crossref
12. NREL [Internet]. [cited 2017 Jan 05]. Available from: Crossref
13. Gebremichael B, Mola GT. The effect of skindepth interfacial defect layer in perovskite solar cell. Applied Physics B. 2016; 122(8):1–8. Crossref
14. Chou TR, Chen SH, Chiang YT, Lina YT, Chao CY. Highly conductive PEDOT:PSS films by post treatment with dimethyl sulfoxide for ITO-free liquid crystal display. Journal of Material Chemistry C. 2015; 3(15):3760–6. Crossref
15. Dimitrieva OP, Grinkoa DA, Noskovb YV, Ogurtsovb NA, Pud AA. PEDOT:PSS films effect of organic solvent additives and annealing on the film conductivity. Synthetic metals. 2009; 159(21):2237–39. Crossref
16. Chen LC, Chen JC, Chen CC, Chun-Guey W. Fabrication and properties of high-efficiency perovskite/PCBM organic solar cells. Nano Scale Research Letters. 2015; 10(312):312–15. Crossref
17. Mahani N. Pseudo-system-level network-on-chipdesign and simulation with VHDL: A comparative case study on simulation time trade-offs. Indian Journal of Science and Technology. 2016 Feb; 9(7):1–7. Crossref
18. Hamid HG. Innovative conceptual design on a tracked robot using TRIZ method for passing narrow obstacles. Indian Journal of Science and Technology. 2016 Feb; 9(7):1–5.
19. Malathi M, Ramar K, Paramasivam C. Obtaining feasible paths with obstacle avoidance using watershed algorithm through simulation. Indian Journal of Science and Technology. 2016 Feb; 9(8):1–9. Crossref
20. Hatem A, Mzoughi D, Arafet B, Adelkader M. Modeling and Simulation of 1.2 kW Nexa PEM Fuel Cell System. Indian Journal of Science and Technology. 2016 Mar,9(9):1-8.
21. Mezaal YS. New compact microstrip patch antennas: Design and simulation results. Indian Journal of Science and Technology. 2016 Mar; 9(12):1–6. Crossref
22. Niemegeers A, Burgelman, Decock, Verschraegen J, Degrave S. SCAPS manual UGent – ELIS; 2013 Sep. p. 1–110.
23. Rutledge SA, Helmy AS. Carrier mobility enhancement in poly(3,4-ethylenedioxythiophene)-poly (styrenesulfonate) having undergone rapid thermal annealing. Journal of Applied Physics. 2013, 114(13):133708-1–5. Crossref
24. MinemotoT, Murata M. Device modelling of perovskite solar cells based on structural similarity with thin film inor-

ganic semiconductor solar cells. Journal of Applied Physics. 2014; 116(5):054501–6. Crossref

25. Shi D, Adinolfi V, Comin R, Yuan M, Alarousu E, Buin A, Chen Y, Hoogland S, Rothenberger A, Katsiev K, Losovyj Y, Zhang X, Dowben PA, Mohammed OF, Sargent EH, Bakr OM. Low trap-state density and long carrier diffusion in organolead trihalide perovskite single crystals. Science. 2015; 347(6221):519–22. Crossref
26. Saidaminov M, Abdelhady AL, Murali B, Alarousu E, Burlakov VM, Peng W, Dursun I, Wang L, He Y, Maculan G, Goriely A, Wu T, Mohammed OF, Bakr OM. High-quality bulk hybrid perovskite single crystals within minutes by inverse temperature crystallization. Nature Communications. 2015; 6(7586):1–6. Crossref
27. Mihailetchi VD, Van Duren JK, Blom PWM, Hummelen JC, Janssen RAJ, Kroon JM, Rispens MT, Verhees WJH, Wienk MM. Electron transport in methanofullerene. Advanced Functional Materials. 2003; 13(1): 43–6. Crossref
28. Yin WJ, Shi TT, Yan YF. Unique properties of halide perovskites as possible origins of the superior solar cell performance. Advanced Materials. 2014 Jul; 26(27):4653–8. Crossref
29. Stoumpos CC, Malliakas CD, Kanatzidis MG. Semiconducting tin and lead iodide perovskites with organic cations: phase transitions, high mobilities, and near-infrared photoluminescent properties. Inorganic Chemistry. 2013; 52(15):9019–38. Crossref
30. Trukhanov VA, Bruevich VV, Paraschuk DY, Effect of doping on performance of organic solar cells. Physics Review B. 2011; 84(20):205–318. Crossref